

Polarization and Electroweak Precision Measurements at the ILC for $\sqrt{s} = 250$ GeV

DPG-Frühjahrstagung, Würzburg

Robert Karl^{1,2}

¹DESY

²Universität Hamburg

22.03.2018



Universität Hamburg

DER FORSCHUNG | DER LEHRE | DER BILDUNG



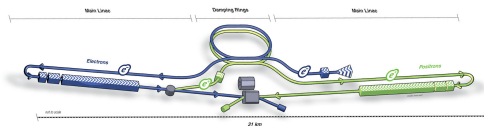
HELMHOLTZ
RESEARCH FOR GRAND CHALLENGES



PIER
Helmholtz
Graduate
School
A Graduate Education Program
of Universität Hamburg
in Cooperation with DESY



The International Linear Collider (ILC)

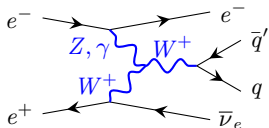


- ▶ Future linear e^+e^- collider:
 $\sqrt{s} = 250 \text{ GeV}$ (As a first stage)
- ▶ Construction under political consideration
in the Kitakami region, Prefecture Iwate, Japan
- ▶ **At the ILC both beams (e^+ , e^-) are polarized:** $P_{e^-} = \pm 80\%$, $P_{e^+} = \pm 30\%$
- ▶ **Switch of polarization sign (helicity reversal) \rightarrow choice of spin configuration**
- ▶ Designed for precision studies for physics of the standard model and beyond

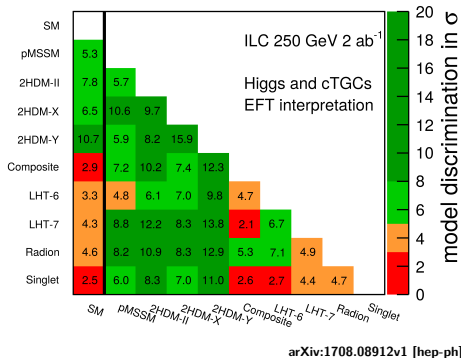
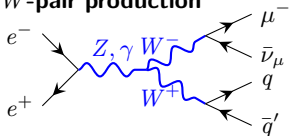


Anomalous Triple Gauge Couplings (aTGCs)

TGC for e.g.:
single W



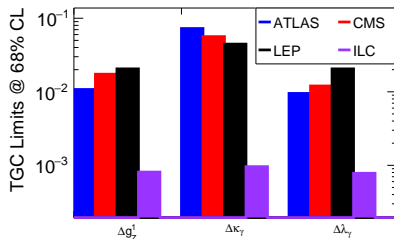
and W -pair production



- ▶ The constraint of TGCs and their precision of $\approx 10^{-3}$ is necessary for the distinction of different Higgs-models beyond the SM
- ▶ Additional bosons (e.g. Z') will affect TGCs
- ⇒ TGCs have to be precisely measured
- ⇒ aTGCs described by an Effective Field Theory (EFT)



Triple Gauge Couplings (TGC)



- ⇒ Polarization has to be known as precisely as the luminosity!
- ⇒ Requirement for a permille-level precision of the luminosity-weighted average polarization

8 TeV ATLAS: 20.3 fb^{-1} ; CMS: 19.4 fb^{-1}

Previously achieved polarization precision

$$\text{HERA: } \Delta P/P = 2\%_{\text{stat}} \oplus 1\%_{\text{sys}} \quad [1]$$

$$\text{SLAC: } \Delta P/P = 1.1\% \quad [2]$$

- ⇒ More than one order of magnitude better precision on both TGC and polarization measurement (for 2 ab^{-2} at 250 GeV)
- ⇒ Accomplished by simultaneous measurement of both of them

Beam Polarization Dependent Cross Section

- Theoretical polarized cross section in general:

$$\begin{aligned}\sigma_{\text{theory}}(P_{e^-}, P_{e^+}) = & \frac{(1-P_{e^-})}{2} \frac{(1-P_{e^+})}{2} \cdot \sigma_{\text{LL}} + \frac{(1+P_{e^-})}{2} \frac{(1+P_{e^+})}{2} \cdot \sigma_{\text{RR}} \\ & + \frac{(1-P_{e^-})}{2} \frac{(1+P_{e^+})}{2} \cdot \sigma_{\text{LR}} + \frac{(1+P_{e^-})}{2} \frac{(1-P_{e^+})}{2} \cdot \sigma_{\text{RL}}\end{aligned}$$

- Nominal ILC polarization values

$$\underbrace{P_{e^-}^- = -80\%}_{\text{"left"-handed } e^- \text{-beam}}$$

$$\underbrace{P_{e^-}^+ = 80\%}_{\text{"right"-handed } e^- \text{-beam}}$$

$$\underbrace{P_{e^+}^- = -30\%}_{\text{"left"-handed } e^+ \text{-beam}}$$

$$\underbrace{P_{e^+}^+ = 30\%}_{\text{"right"-handed } e^+ \text{-beam}}$$

- Cross section of the 4 polarization configurations

$$\sigma_{--} := \sigma(P_{e^-}^-, P_{e^+}^-)$$

$$\sigma_{++} := \sigma(P_{e^-}^+, P_{e^+}^+)$$

$$\sigma_{-+} := \sigma(P_{e^-}^-, P_{e^+}^+)$$

$$\sigma_{+-} := \sigma(P_{e^-}^+, P_{e^+}^-)$$

- $\sigma_{\text{LL}}, \sigma_{\text{RR}}, \sigma_{\text{LR}}, \sigma_{\text{RL}}$ are theoretically calculated including Initial State Radiation (ISR) and beam spectrum



- ▶ Measured polarized cross section:

$$\sigma_{\text{data}} = \frac{D - \mathfrak{B}}{\varepsilon \cdot \mathcal{L}}$$

D : Number of selected events

\mathfrak{B} : Background expectation value

ε : Detector selection efficiency

\mathcal{L} : Integrated luminosity

Remark:

All of them can vary between the different data sets (σ_{-+} , σ_{+-} , σ_{--} , σ_{++})

- ▶ Uncertainty of the polarized cross section is calculated via error propagation

Remark:

Statistical uncertainty is always uncorrelated: $\text{corr}(\sigma_i^D, \sigma_j^D) \equiv \delta_{ij}$

And it is determined by Poisson fluctuations: $\Delta D \equiv \sqrt{D}$

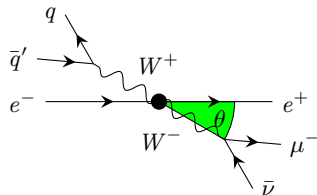


Usage of the Differential Polarized Cross Section

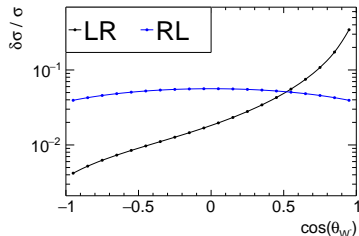
e.g.: $e^+e^- \rightarrow W^+W^- \rightarrow q\bar{q}'\mu^-\bar{\nu}$

Choice of the angle:

- ✓ Individual for each channel
- ✓ High dependence of the angular distribution on the chiral structure
- ✓ Angle has to be well measurable
- ✓ Multi-angle distribution available



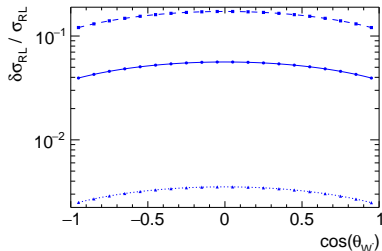
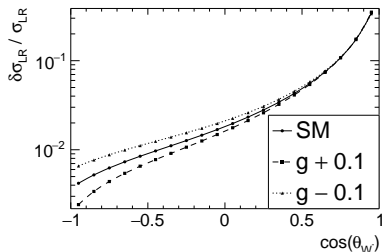
Projection on the θ_{W^-} -axis



Bin-wise cross section calculation:

- ▶ Cross section calculated for each bin:
 - Labeled for the i -th bin as $\delta_i\sigma$
- ▶ Analog for the selected events, background and selection efficiency
 - Calculated bin-wise

Effect of Anomalous TGC in $e^-e^+ \rightarrow \mu\nu q\bar{q}$ at 250 GeV



► The effect of the TGC g on the angular distribution

- Variation the TGC within $\pm 10\%$ corresponds to $\pm 5\sigma$ deviation at LEP

⇒ Only a very small impact on the angular distribution

⇒ Especial sensitive only for ranges of low differential cross sections

► Precision measurement of TGCs:

- A clear angular dependence: Event rates are affected simultaneously over the full angular range

+ Strong dependence of the chiral structure

► Considered Channels and their Parameters:

channel	cross section	left-right asymmetry	TGC
$e^- e^+ \longrightarrow e^- \bar{\nu} q \bar{q}$	$\sigma_{e^- \bar{\nu} q \bar{q}}$	$A_{RR}^{e^- \bar{\nu} q \bar{q}} = \frac{\sigma_{LR} - \sigma_{RR}}{\sigma_{LR} + \sigma_{RR}}$	$g_Z^1, \kappa_\gamma, \lambda_\gamma$
$e^- e^+ \longrightarrow e^+ \nu q \bar{q}$	$\sigma_{e^+ \nu q \bar{q}}$	$A_{LL}^{e^+ \nu q \bar{q}} = \frac{\sigma_{LR} - \sigma_{LL}}{\sigma_{LR} + \sigma_{LL}}$	$g_Z^1, \kappa_\gamma, \lambda_\gamma$
$e^- e^+ \longrightarrow \mu \nu q \bar{q}$	$\sigma_{\mu \nu q \bar{q}}$	$A_{RL}^{\mu \nu q \bar{q}} = \frac{\sigma_{LR} - \sigma_{RL}}{\sigma_{LR} + \sigma_{RL}}$	$g_Z^1, \kappa_\gamma, \lambda_\gamma$
$e^- e^+ \longrightarrow \mu^+ \mu^- q \bar{q}$	$\sigma_{\mu \mu q \bar{q}}$	$A_{RL}^{\mu \mu q \bar{q}} = \frac{\sigma_{LR} - \sigma_{RL}}{\sigma_{LR} + \sigma_{RL}}$	–
$e^- e^+ \longrightarrow q \bar{q}$	$\sigma_{q \bar{q}}$	$A_{RL}^{q \bar{q}} = \frac{\sigma_{LR} - \sigma_{RL}}{\sigma_{LR} + \sigma_{RL}}$	–
$e^- e^+ \longrightarrow l l$	σ_{ll}	$A_{RL}^{ll} = \frac{\sigma_{LR} - \sigma_{RL}}{\sigma_{LR} + \sigma_{RL}}$	–

► $P_{e^-}^-, P_{e^-}^+, P_{e^+}^-, P_{e^+}^+$ determined globally for all channels

► Using the method of least squares:

$$\chi^2 = \sum_{\text{channel}} \left[\sum_{\text{bin } i} (\delta_i \vec{\sigma}_{\text{data}} - \delta_i \vec{\sigma}_{\text{theory}})^T (\delta_i \Xi)^{-1} (\delta_i \vec{\sigma}_{\text{data}} - \delta_i \vec{\sigma}_{\text{theory}}) \right];$$

$$\vec{\sigma} := \left(\delta_i \sigma_{-+} \quad \delta_i \sigma_{+-} \quad \delta_i \sigma_{--} \quad \delta_i \sigma_{++} \right)^T$$

Results

Using the following
global parameter values:

$$\varepsilon = 0.6$$

$$\pi = \frac{D - \mathfrak{B}}{D} = 0.8$$

$$\mathcal{L} = 2 \text{ ab}^{-1}$$

$$\Delta\varepsilon = \Delta\pi = \Delta\mathcal{L} = 0$$

Luminosity sharing:

$$\begin{aligned} -+ : 45\%, \quad +- : 45\%, \\ -- : 5\%, \quad ++ : 5\% \end{aligned}$$

All results are in the order
of 10^{-3} !

Cross Section [10^{-4}]

$\Delta\sigma_{e^+\nu q\bar{q}}/\sigma$	12.9
$\Delta\sigma_{e^-\bar{\nu} q\bar{q}}/\sigma$	13.3
$\Delta\sigma_{\mu\nu q\bar{q}}/\sigma$	11.4
$\Delta\sigma_{\mu\mu q\bar{q}}/\sigma$	13.8
$\Delta\sigma_{q\bar{q}}/\sigma$	3.78
$\Delta\sigma_{ll}/\sigma$	3.91

Asymmetry [10^{-4}]

$\Delta A_{RR}^{e^+\nu q\bar{q}}$	6.37
$\Delta A_{LL}^{e^-\bar{\nu} q\bar{q}}$	19.1
$\Delta A_{LR}^{\mu\nu q\bar{q}}$	3.32
$\Delta A_{LR}^{\mu\mu q\bar{q}}$	15.4
$\Delta A_{LR}^{q\bar{q}}$	6.66
ΔA_{LR}^{ll}	7.72

Polarization [10^{-4}]

$\Delta P_{e^-}^-$	7.68
$\Delta P_{e^-}^+$	3.4
$\Delta P_{e^+}^-$	8.11
$\Delta P_{e^+}^+$	10.7

TGC [10^{-4}]

Δg	8.18
$\Delta\kappa$	10.1
$\Delta\lambda$	9.33

- ▶ **Polarization provides a deep insight into the chiral structure of the standard model and beyond**
 - ▶ A permille-level precision of the luminosity-weighted average polarization at the IP is required
- ▶ **A full electroweak precision fit is achievable at the ILC**
 - ▶ The beam polarization, unpolarized cross section, the left-right asymmetry and anomalous Triple Gauge couplings can be determined with a relative precision of $\mathcal{O}(10^{-3})$
- ▶ **Additional studies on the dependence of systematic quantities and their uncertainties will follow**



- [1] S. Baudrand, M Bouchela, V Brissona, R Chichea, M Jacqueta, S Kurbasova, G Lia, C Pascauda, A Rebouxa, V Soskova, Z Zhanga, F Zomera, M Beckinghamb, T Behnkeb, N Coppolab, N Meynersb, D Pitzlb, S Schmittb, M Authierc, P Deck-Betinellic, Y Queinecc and L Pinardd, *A high precision Fabry-Perot cavity polarimeter at HERA*, Journal of Instrumentation 2010,
(<http://www.slac.stanford.edu/cgi-wrap/getdoc/slac-pub-6700.pdf>)
- [2] P. C. ROWSON, *PRECISION ELECTROWEAK PHYSICS WITH THE SLD/SLC: THE LEFT-RIGHT POLARIZATION ASYMMETRY*, SLAC-PUB-6700, December 1994,
(<http://www.slac.stanford.edu/cgi-wrap/getdoc/slac-pub-6700.pdf>)



Backup Slides



Polarized Cross Section Measurement

- Measured polarized cross section:

$$\sigma_{\text{data}} = \frac{D - \mathfrak{B}}{\varepsilon \cdot \mathcal{L}}$$

D : Number of selected events

\mathfrak{B} : Background expectation value

ε : Detector selection efficiency

\mathcal{L} : Integrated luminosity

Remark:

All of them can vary between the different data sets (σ_{-+} , σ_{+-} , σ_{--} , σ_{++})

- Uncertainty of the polarized cross section is calculated via error propagation

$$\text{e.g. } (\Xi_{\mathcal{L}})_{ij} = \text{corr}(\sigma_i^{\mathcal{L}}, \sigma_j^{\mathcal{L}}) \frac{\partial \sigma_i}{\partial \mathcal{L}_i} \frac{\partial \sigma_j}{\partial \mathcal{L}_j} \Delta \mathcal{L}_i \Delta \mathcal{L}_j \quad i, j \in \{-+, +-, --, ++\}$$

$$\Xi := \underbrace{\Xi_D}_{\text{statistical uncertainty}} + \underbrace{\Xi_{\mathfrak{B}} + \Xi_{\varepsilon} + \Xi_{\mathcal{L}}}_{\text{systematic uncertainty}};$$

Remark:

Statistical uncertainty is always uncorrelated: $\text{corr}(\sigma_i^D, \sigma_j^D) \equiv \delta_{ij}$

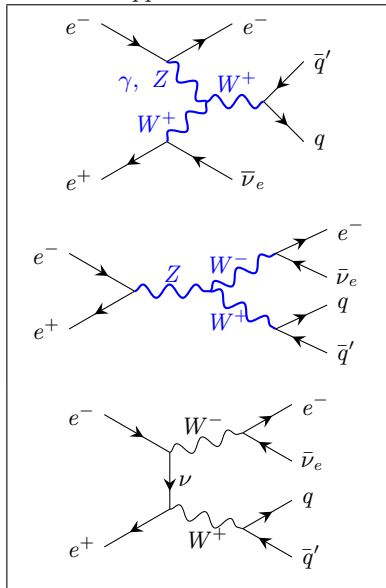
And it is determined by Poisson fluctuations:

$$\Delta D \equiv \sqrt{D}$$

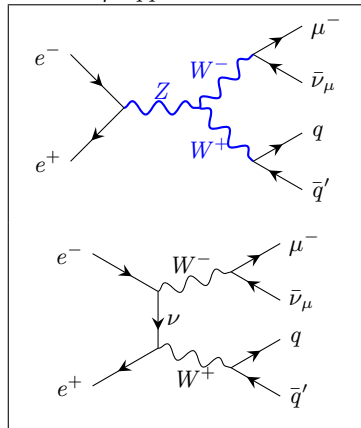


TGC Contribution for the Final State

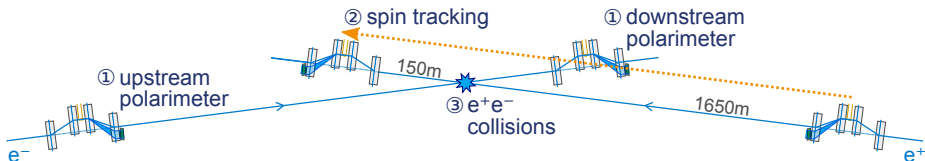
$$e^+e^- \rightarrow e\nu q\bar{q}$$



$$e^+e^- \rightarrow \mu\nu q\bar{q}$$



ILC Polarimetry Concept for Per mille-Level Polarization Precision



► The time-resolved beam polarization:

- Measured with 2 laser-Compton polarimeters before and after the e^-e^+ IP
- Polarimeter precision $\Delta P/P = 0.25\%$ from the start
- Extrapolated to the e^-e^+ IP via spin tracking

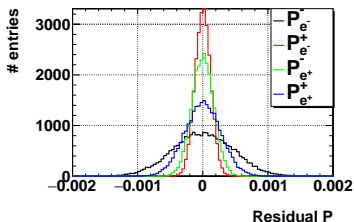
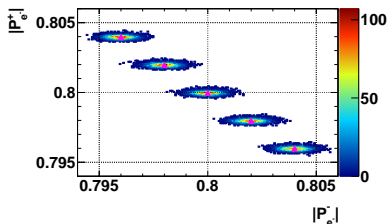
+ The luminosity-weighted averaged polarization:

- Calculated from collision data at the IP
- Using the cross section measurement of well known standard model processes

⇒ Combination of both measurements

- With the aim to reach the permille-level precision $\Delta P/P = 0.1\%$

Testing for a Non-Perfect Helicity Reversal



► Variation in the absolute polarization

- Toy Measurement for 5 different polarization discrepancies for both beams
- Nominal initial polarizations: $|P_{e^-}| = 80\%$, $|P_{e^+}| = 30\%$
- Statistical uncertainties only

► χ^2 -Fit:

- Correct determination of the 4 polarization values
- No noticeable impact on polarization precision using total cross sections

✓ **Can compensate for a non-perfect helicity reversal**

Consider Constraints from the Polarimeter Measurement

Simplified approach: (as a first step)

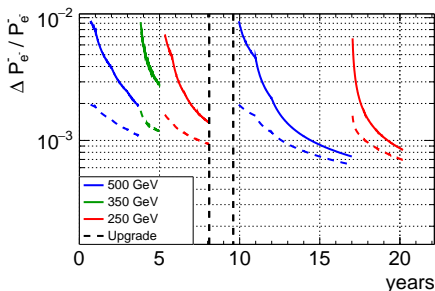
- ▶ Neglect spin transport
- ▶ Using $\Delta P/P = 0.25\%$:
- ▶ Gaussian distribution
 - ▶ Mean: $|P_{e-}| = 80\%, |P_{e+}| = 30\%$
 - ▶ Width: ΔP

Implementation:

$$\chi'^2 = \chi^2 + \sum_P \left[\frac{(P_{e\pm}^\pm - \mathcal{P}_{e\pm}^\pm)^2}{\Delta \mathcal{P}^2} \right]$$

- ▶ $P_{e\pm}^\pm$: 4 fitted parameters
- ▶ $\mathcal{P}_{e\pm}^\pm$: Polarimeter measurement
- ▶ $\Delta \mathcal{P}$: Polarimeter uncertainty

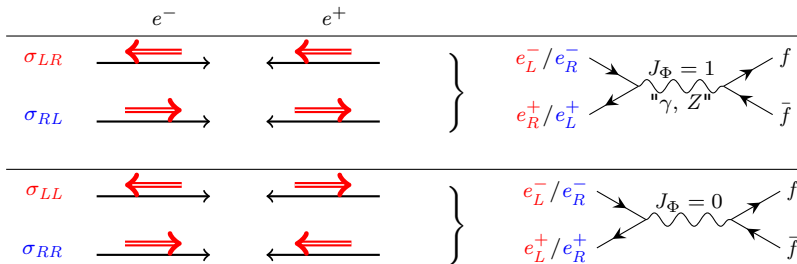
$E[\text{GeV}]$	500	350	250	500	250
$\mathcal{L}[1/\text{fb}]$	500	200	500	3500	1500
$[10^{-3}]$	Without Constraint				
$\Delta P_{e-}^-/P$	1.9	2.8	1.4	0.74	0.84
$[10^{-3}]$	With Constraint				
$\Delta P_{e-}^-/P$	1.1	1.2	0.93	0.63	0.69



Polarization at an e^-e^+ Collider

► Consider only one electron positron pair:

- Helicity is the projection of the spin vector on the direction of motion
- In case of massless particles, helicity is equal to chirality (left and right handedness)
- If $E_{\text{kin}} \gg E_0 \rightarrow m_e \approx 0$ e.g. ILC: $E_{\text{kin}}/E_0 \approx \mathcal{O}(10^5 - 10^6)$



► For a bunch of particles the polarization P is defined as:

$$P := \frac{N_R - N_L}{N_R + N_L} \quad \begin{cases} N_R : & \text{The number of right-handed particles} \\ N_L : & \text{The number of left-handed particles} \end{cases}$$

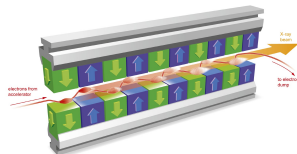
Production of Polarized Beams

Electron beam:

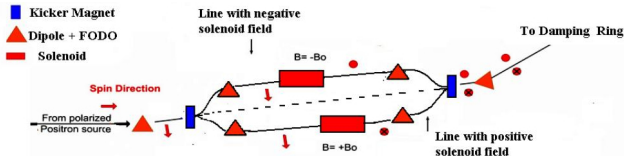
- ▶ Shooting of a circular polarized laser on a photocathode
- ▶ Switch between polarization signs (helicity reversal)
 - ⇒ Switch between signs of the laser polarization

Positron beam:

- ▶ Production of circular polarized γ 's from e^- -beam propagating through a helical undulator
 - ⇒ e^+ obtained via pair-production of the γ 's
- ▶ Helicity reversal
 - ⇒ Switch between two beam lines



www.xfel.eu/ueberblick/funktionsweise/



Laser-Compton Polarimeters

Spin Tracking

Collision Data

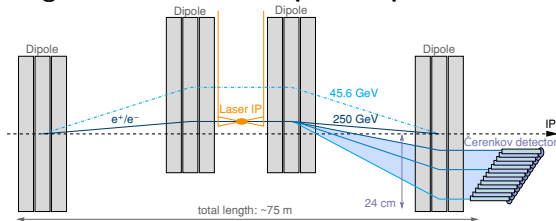
Improvement by Constraints from Polarimeter Measurement

Outlook



Laser-Compton Polarimeters

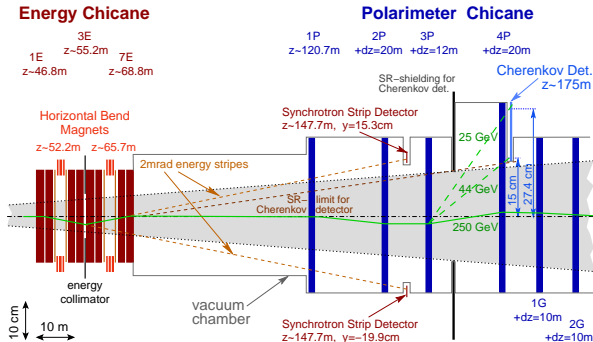
Magnetic chicane of the upstream polarimeters



- ▶ Compton scattering of the beam with a polarized Laser
- ▶ $\mathcal{O}(10^3)$ particles per bunch ($2 \cdot 10^{10}$) are scattered
- ▶ Magnetic chicane:
energy spectrum
⇒ spatial distribution

- ▶ Energy spectrum measurement:
⇒ Counting the scattered particles at different positions
- ▶ Design of the magnetic Chicane:
 - ▶ Laser-bunch interaction point moves with beam energy
→ position of the Compton edge stays the same
 - ▶ Orbit of the non-scattered particles is unaffected by the magnetic chicane

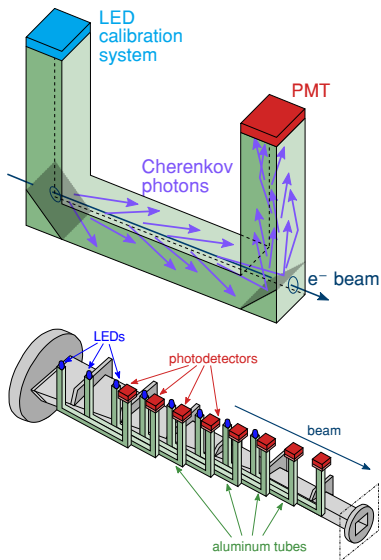
Downstream Polarimeter



Difference to Upstream Polarimeter due to a large disturbed beam

- ▶ Stronger banding of the beam after γ -IP
- ▶ 2 additional magnets to restore the beam orbit
- ▶ Measuring one bunch per train

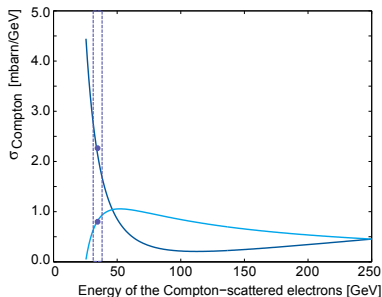
Cherenkov Detectors: Basic Concept



- ▶ U-shape channels filled with gas:
e.g. perfluorobutane
- ▶ Concept
 - ▶ Scattered particles propagate through the bottom
 - ▶ Produced Cherenkov light is reflected to one end of the channel
 - ▶ Light measurement with photomultiplier tube (PMT)
- ▶ At the other end: LED for PMT calibration
- ▶ Sampling of the energy distribution
→ Number of Cherenkov detector
- ▶ Energy resolution
→ Thickness of a Cherenkov detector
- ▶ Quartz Cherenkov detector concept:
Ref.: Theses Annika Vauth

<http://bib-pubdb1.desy.de/record/171400>

Differential Compton Cross Section



Energy dependence:

$$\frac{d\sigma_C}{dy_C} = \frac{2\pi r_e^2}{x_C} (a_C + \lambda \mathcal{P} \cdot b_C); \quad y_C := 1 - \frac{E'}{E}$$

e^- Polarization: \mathcal{P} ; Laser Polarization: λ

DarkBlue: $\lambda \mathcal{P} = +1$

Cyan: $\lambda \mathcal{P} = -1$

Calculating \mathcal{P}_i of the i -th channel with asymmetry A_i , analysing power Π_i

$$A_i := \frac{N_i^- - N_i^+}{N_i^- + N_i^+}; \quad \Pi_i = \frac{\mathcal{I}_i^- - \mathcal{I}_i^+}{\mathcal{I}_i^- + \mathcal{I}_i^+}; \quad \mathcal{I}_i^\pm := \int_{E_i - \Delta/2}^{E_i + \Delta/2} \frac{d\sigma_C}{dy_C} \Big|_{\lambda \mathcal{P} = \pm 1} dy_C$$

$N^\pm := \#e_{\text{Compton}}$ for $\lambda \mathcal{P} = \pm 1$; E_i : energy of i -th channel; Δ : energy width

$$\Rightarrow \lambda \mathcal{P}_i = \frac{A_i}{\Pi_i} \quad \Rightarrow \quad \mathcal{P} = \langle \mathcal{P}_i \rangle$$

Compton Scattering Cross Section: Formulary

$$\frac{d\sigma}{dy_C} = \frac{2\pi r_e^2}{x_C} (a_C + \lambda \mathcal{P} \cdot b_C)$$

$$y_C := 1 - \frac{E'_\gamma}{E}; \quad x_C := \frac{4EE_\gamma}{m_e^2} \cos^2\left(\frac{\vartheta_0}{2}\right)$$

$$r_C := \frac{y_C}{x_C(1 - y_C)}$$

$$a_C := (1 - y_C)^{-1} + 1 - y_C - 4r_C(1 - r_C)$$

$$b_C := r_C x_C (1 - 2r_C)(2 - y_C)$$

E, E_γ : e^-, γ energy before Compton scattering

E', E'_γ : e^-, γ energy after Compton scattering

m_e, r_e : mass, classical radius of e^-

ϑ_0 : crossing angle between e^-, γ

\mathcal{P} : longitudinal polarization of e^-

λ : circular polarization of γ_{Laser}

Characteristic Point:

$$E'_{\text{crossover}} = \frac{E}{1 + x_C/2},$$

$$E'_{\text{ComptonEdge}} = E'_{\text{min}} = \frac{E}{1 + x_C}$$

Laser-Compton Polarimeters

Spin Tracking

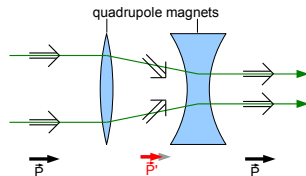
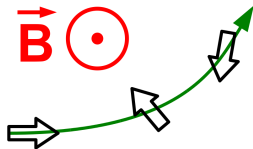
Collision Data

Improvement by Constraints from Polarimeter Measurement

Outlook



Spin Precession



- ▶ Polarimeters are 1.65 km and 150 m away from IP
 - Particles propagate through magnets
 - Magnets influence the spin, as well
 - Described by Thomas precession

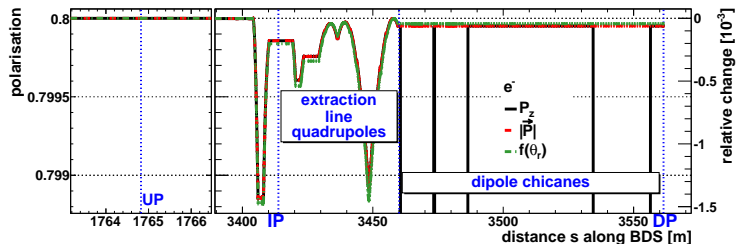
- ▶ if $\vec{B}_{\parallel} = \vec{E} = 0$:

$$\frac{d}{dt} \vec{S} = -\frac{q}{m\gamma} \left((1 + a\gamma) \vec{B}_{\perp} \right) \times \vec{S}$$

- ▶ Effects from focusing and defocusing can cancel
- ▶ For a series of quadrupole magnets \mathcal{P} described by the angular divergence θ_r

$$f(\theta_r) = |\vec{\mathcal{P}}|_{\max} \cdot \cos((1 + a\gamma) \cdot \theta_r)$$

Spin Tracking



Further causes of longitudinal beam polarization change:

- ▶ *Bremsstrahlung*:
Deceleration by passing through matter → negligible for colliders
- ▶ *Beamstrahlung*:
Deflection by the em-field of the oncoming bunch during collision
- ▶ *Synchrotron radiation*:
Deflection by the em-field of accelerator magnets

Systematic Polarization Uncertainty

contribution	uncertainty [10^{-3}]
Beam and polarization alignment at polarimeters and IP ($\Delta\vartheta_{\text{bunch}} = 50 \mu\text{rad}$, $\Delta\vartheta_{\text{pol}} = 25 \text{ mrad}$)	0.72
Variation in beam parameters (10 % in the emittances)	0.03
Bunch rotation to compensate the beam crossing angle	< 0.01
Longitudinal precession in detector magnets	0.01
Emission of synchrotron radiation	0.005
Misalignments (10μ) without collision effects	0.43
Total (quadratic sum)	0.85
Collision effects in absence of misalignments	< 2.2

[Ref.:] Thesis Moritz Beckmann (<http://bib-pubdb1.desy.de/record/155874>)



Laser-Compton Polarimeters

Spin Tracking

Collision Data

Consider Angular Information by Using differential Cross Section

Improvement by Constraints from Polarimeter Measurement

Outlook



χ^2 -Minimization

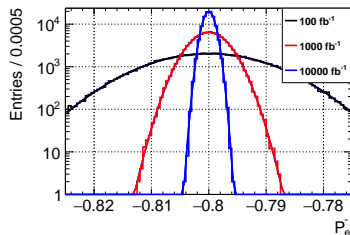
► Defining χ^2 function:

$$\chi^2 := \sum_{\text{process}} \sum_{\pm\pm} \frac{(\sigma_{\text{data}} - \sigma_{\text{theory}}(P_{e^-}^-, P_{e^-}^+, P_{e^+}^-, P_{e^+}^+))^2}{\Delta\sigma^2}$$

► Varying $(P_{e^-}^-, P_{e^-}^+, P_{e^+}^-, P_{e^+}^+)$ \rightarrow Minimizes χ^2

► Toy measurement:

- Signal expectation value:
 $\langle D \rangle = \sigma_{\text{theory}} \cdot \varepsilon \cdot \mathcal{L} + \mathfrak{B}$
- One toy experiment:
 Random Poisson number around each $\langle D \rangle$
- Determine $P_{e^\pm}^\pm$ by minimizing χ^2
- Simplified case for illustration:
 - $\mathfrak{B} = 0$ and $\varepsilon = 1$
 - Statistical uncertainties only
 - Using 10^5 toy measurements

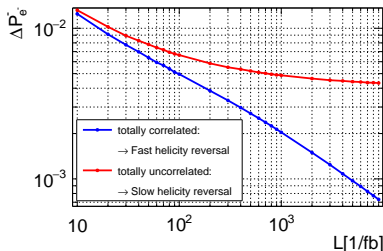


Systematic Uncertainties and their Correlations

▶ Systematic Uncertainties are influenced by

- ▶ Detector calibration and alignment
- ▶ Machine performance
- ▶ ...

⇒ Time dependent uncertainties



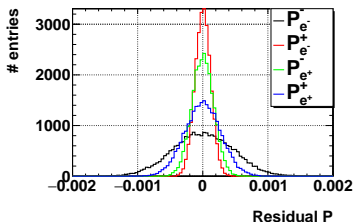
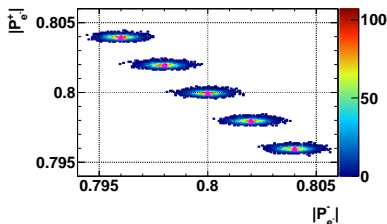
▶ Data set are taken one at a time:

- ▶ Slow frequency of helicity reversals: \mathcal{O} (weeks to months)
- ▶ Data sets are independent
- Completely uncorrelated
- ✗ Lead to saturation at systematic precision

▶ Data sets taken concurrently:

- ▶ Fast frequency of helicity reversals: \mathcal{O} (train-by-train)
- Faster than changes in calibration/alignment
- Generate correlations
- ✓ Lead to cancellation of systematic uncertainties

Testing for a Non-Perfect Helicity Reversal



► Variation in the absolute polarization

- Toy Measurement for 5 different polarization discrepancies for both beams
- Nominal initial polarizations: $|P_{e-}| = 80\%$, $|P_{e+}| = 30\%$
- Statistical uncertainties only

► χ^2 -Fit:

- Correct determination of the 4 polarization values
- No noticeable impact on polarization precision using total cross sections

✓ **Can compensate for a non-perfect helicity reversal**

Theoretical Limit of the Statistical Precision

Consider most relevant processes:

Process	Channel
single W^\pm	$e\nu l\nu, e\nu q\bar{q}$
WW	$q\bar{q}q\bar{q}, q\bar{q}l\nu, l\nu l\nu$
ZZ	$q\bar{q}q\bar{q}, q\bar{q}ll, ll ll$
$ZZWW$ Mix	$q\bar{q}q\bar{q}, l\nu l\nu$
Z	$q\bar{q}, ll$

- ▶ Same processes as for physics analysis (DBD)
- ▶ Tree-level cross sections + ISR
- ▶ Any combination of processes can be used
- ▶ Further process can easily added

Consider best case scenario using σ_{tot} :

- ▶ Assumption of a perfect 4π detector
- ▶ No background
- ▶ No systematic uncertainties
- ▶ Using all considered processes

Statistical precision H-20: $\Delta P/P$ [%]

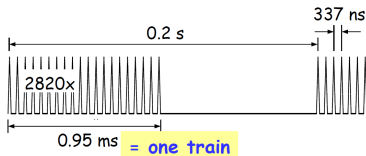
E	500	350	250	500	250
\mathcal{L}	500	200	500	3500	1500
P_{e-}^-	0.2	0.3	0.1	0.08	0.09
P_{e-}^+	0.05	0.06	0.03	0.02	0.02
P_{e+}^-	0.1	0.1	0.06	0.04	0.04
P_{e+}^+	0.2	0.3	0.1	0.08	0.08

Generation of Correlated Uncertainties: Fast Helicity Reversal

Generation of Correlated Uncertainties

- ⇒ Change between data sets (σ_{-+} , σ_{+-} , σ_{--} , σ_{++}) faster than change in detector and accelerator calibration
- ⇒ Change between data sets during normal run without additional breaks

ILC Bunch Structure

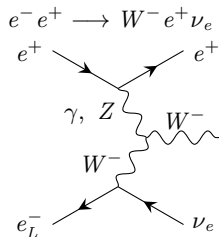
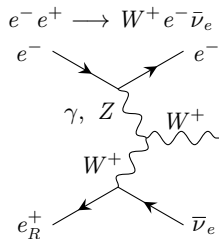


Two possible frequency:

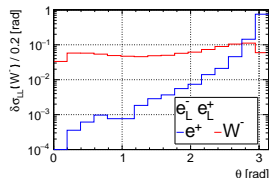
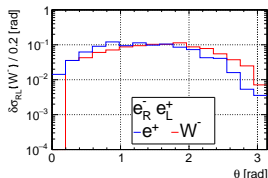
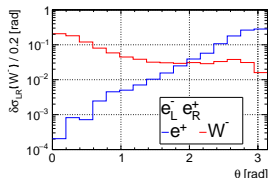
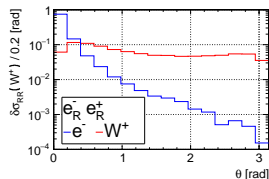
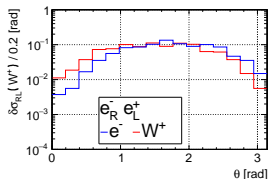
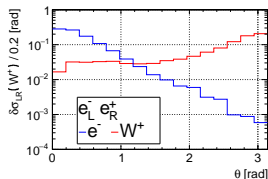
- ▶ bunch-by-bunch: switch between two bunches
 - ▶ train-by-train: switch between two trains
- ▶ Technical feasibility much easier for train-by-train
 - ▶ Switch train-by-train should be sufficient for polarization precision
- ⇒ Precise correlation coefficient still to do

Consideration of the Addition Information from the Angular Distribution

- ▶ Total cross section
 - ▶ Rely on theoretical calculation
 - ⇒ Susceptible to BSM effects
- ▶ Differential cross section
 - ▶ Additional usage of the angular information
 - ⇒ Increase of the robustness against BSM effects
- ▶ Starting with Single W Process
 - ▶ Angular distribution has a large dependence on the chirality
 - ▶ Separated in W^+ and W^- production
 - ⇒ Sensitive to individual beam polarization
 - ▶ W^+ : only sensitive to P_{e+}
 - ▶ W^- : only sensitive to P_{e-}
- ▶ Further processes can easily be included



Single W^\pm : Polar Production Angle Distribution



► Single differential cross section: $\partial\sigma/\partial\theta$

- Two independent angles: θ_e , θ_W
- For now start with $\theta_e \rightarrow e^\pm$ also needed for separation between W^\pm

► $\partial\sigma/\partial\theta$ will be calculated via $\Delta\sigma_i/\Delta\theta_i$ ("cross section for the i -th bin in θ ")

Usage of the Differential Polarized Cross Section

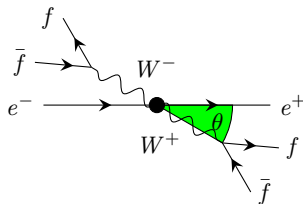
► Total cross section

- Rely on theoretical calculation
- ⇒ Susceptible to BSM effects

► Differential cross section

- Additional usage of the angular information
- ⇒ Increase of the robustness against BSM effects

e.g.: $e^+e^- \rightarrow W^+W^- \rightarrow q\bar{q}l\nu$

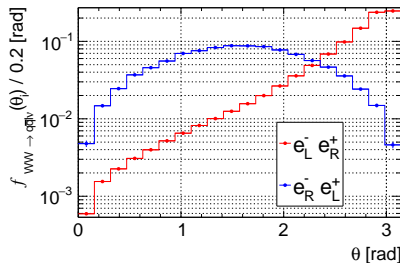


Bin-wise cross section calculation:

$$\begin{aligned} \underbrace{\frac{\partial \sigma}{\partial \theta}}_{\text{differential cross section}} &\longrightarrow \underbrace{\delta_i \sigma_{\text{data}}}_{\text{cross section of the } i\text{-th bin}} := \delta_i N / \mathcal{L} \\ &\longrightarrow \delta_i \sigma_{LR} := f_{LR}(\theta_i) \cdot \sigma_{LR} \end{aligned}$$

Analog: RL , LL , RR

- $\delta_i N$: events of i -th bin
- $f(\theta_i)$: fraction of the total cross section



Defining Differential Cross Sections

Measured cross section:

$$\overbrace{\frac{\partial \sigma}{\partial \theta}}^{\text{differential cross section}} \longrightarrow \overbrace{\delta_i \sigma_{\text{data}}}^{\text{cross section per } i\text{th bin}} := \frac{\delta_i D - \delta_i \mathfrak{B}}{\delta_i \varepsilon \cdot \mathcal{L}}$$

$$\left. \begin{array}{ll} \delta_i D & \text{Number of signal events} \\ \delta_i \mathfrak{B} & \text{Number of expected background events} \\ \delta_i \varepsilon & \text{Selection efficiency} \\ \mathcal{L} & \text{Integrated luminosity} \end{array} \right\} \text{ of the } i\text{th bin}$$

Theoretical cross section:

$$\begin{aligned} \delta_i \sigma_{\pm\pm} &= \frac{\binom{1 \pm |P_{e-}^{\pm}|}{2}}{\binom{1 \pm |P_{e+}^{\pm}|}{2}} \delta_i \sigma_{RR} + \frac{\binom{1 \mp |P_{e-}^{\pm}|}{2}}{\binom{1 \mp |P_{e+}^{\pm}|}{2}} \delta_i \sigma_{LL} \\ &+ \frac{\binom{1 \pm |P_{e-}^{\pm}|}{2}}{\binom{1 \mp |P_{e+}^{\pm}|}{2}} \delta_i \sigma_{RL} + \frac{\binom{1 \mp |P_{e-}^{\pm}|}{2}}{\binom{1 \pm |P_{e+}^{\pm}|}{2}} \delta_i \sigma_{LR} \\ \delta_i \sigma_{\text{theory}} &:= f(\theta_i) \cdot \sigma_{\text{theory}} \end{aligned}$$

$f(\theta_i)$ is directly obtained from the angular distributions

Implementing Differential Cross Sections in the χ^2 Minimization

Replacing: $\sigma \longrightarrow \delta_k \sigma + \text{Sum over all bins}$

$$\chi^2 = \sum_{\text{process}} \sum_{\theta_k} (\delta_k \vec{\sigma}_{\text{data}} - \delta_k \vec{\sigma}_{\text{theory}})^T (\delta_k \Xi)^{-1} (\delta_k \vec{\sigma}_{\text{data}} - \delta_k \vec{\sigma}_{\text{theory}})$$

$$\delta_k \vec{\sigma} := \begin{pmatrix} \delta_k \sigma_{-+} & \delta_k \sigma_{+-} & \delta_k \sigma_{--} & \delta_k \sigma_{++} \end{pmatrix}^T$$

$$\delta_k \Xi := \delta_k \Xi_N + \delta_k \Xi_{\mathfrak{B}} + \delta_k \Xi_{\varepsilon} + \delta_k \Xi_{\mathcal{L}};$$

$$(\delta_k \Xi_{\varepsilon})_{ij} = \text{corr}(\vec{\sigma}_i^{\varepsilon}, \vec{\sigma}_j^{\varepsilon}) \frac{\partial (\delta_k \vec{\sigma}_i)}{\partial (\delta_k \varepsilon_i)} \frac{\partial (\delta_k \vec{\sigma}_j)}{\partial (\delta_k \varepsilon_j)} \Delta(\delta_k \varepsilon_i) \Delta(\delta_k \varepsilon_j)$$

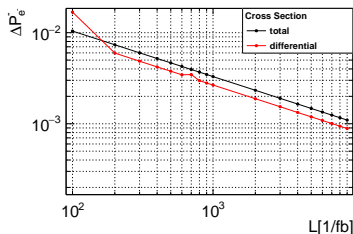
Remarks:

- ▶ Due to correlations, the binning in θ has to be equal for all cross sections
- ▶ It can differ between processes and decay-channels
- ▶ Range and number of bins of θ can be changed externally for each process



First Toy Measurements: Preliminary Results

Single W^\pm only



Using the following configuration:

- ▶ Using 16 equal bins in a θ range of $[0, \pi]$
- ▶ Signal determination bin-by-bin:

$$\langle \delta_k D \rangle = \delta_k \sigma_{\text{theory}} \cdot \delta_k \varepsilon \cdot \mathcal{L} + \delta_k \mathfrak{B}$$
- ▶ For the start:
 Statistical error only + no background
- ▶ Using H-20 integrated luminosity sharing due to energy

- ▶ Differential cross section have a lower statistic uncertainty:
 - ▶ Expectation of $\delta_k D$ can be for some bins $\mathcal{O}(1)$
 - ▶ Some zero diagonal entries of the covariance matrix \rightarrow not invertible
 - \Rightarrow Dropping χ^2 -terms with $\delta_k D = 0$
- ▶ Further steps:
 - ▶ Optimizing the θ range and binning
 - ▶ Including further processes